CrossMark

SCIENTIFIC ARTICLE

MRI of the anterior talofibular ligament, talar cartilage and os subfibulare: Comparison of isotropic resolution 3D and conventional 2D T2-weighted fast spin-echo sequences at 3.0 T

Jisook Yi[1] · Jang Gyu Cha[1] · Young Koo Lee[2] · Bo Ra Lee[3] · Chan Hong Jeon[4]

Abstract

Purpose To determine the accuracy of a three-dimensional (3D) T2-weighted fast spin-echo (FSE) magnetic resonance (MR) sequence compared with two-dimensional (2D) sequence for diagnosing anterior talofibular ligament (ATFL) tears, chondral lesion of the talus (CLT) and os subfibulare/avulsion fracture of the distal fibula (OSF).

Materials and Methods Thirty-five patients were included, who had undergone ankle MRI with 3D T2-weighted FSE and 2D T2-weighted FSE sequences, as well as subsequent ankle arthroscopy, between November 2013 and July 2014. Each MR imaging sequence was independently scored by two readers retrospectively for the presence of ATFL tears, CLT and OSF. The area under the receiver operating curve (AUC) was compared to determine the discriminatory power of the two image sequences. Interobserver agreement was expressed as unweighted kappa value.

Results Arthroscopic findings confirmed 21 complete tears of the ATFL, 14 partial tears of the ATFL, 17 CLTs and 7 OSFs. There were no significant differences in the diagnoses of ATFL tears ($p = 0.074$–0.501), CLT ($p = 0.090$–0.450) and OSF ($p = 0.317$) obtained from the 2D and 3D sequences by either reader. The interobserver agreement rates between two readers using the 3D T2-weighted FSE sequence versus those obtained with the 2D sequence were substantial ($\kappa = 0.659$) versus moderate ($\kappa = 0.553$) for ATFL tears, moderate ($\kappa = 0.499$) versus substantial ($\kappa = 0.676$) for CLT and substantial ($\kappa = 0.621$) versus substantial ($\kappa = 0.689$) for OSF.

Conclusion Three-dimensional isotropic T2-weighted FSE MRI of the ankle resulted in no statistically significant difference in diagnostic performance compared to two-dimensional T2-weighted FSE MRI in the evaluation of ATFL tears, CLTs and OSFs.

Introduction

The ankle is the second most commonly injured joint in athletes (after the knee) [1]. The anterior talofibular ligament (ATFL) is frequently injured during inversion stress of the ankle joint, which can lead to lateral instability of the joint [2]. Furthermore, chondral lesion of the talus (CLT) is a common articular lesion of the ankle and frequently occurs in response to repetitive stress, hereditary ossification defects, abnormal stress due to malalignment and microemboli with peripheral necrosis of bone; it is usually traumatic in origin [3]. Most patients with CLT have chronic pain of the ankle joint, which seriously limits daily life as well as sporting activities [4]. The os subfibulare is an accessory bone located under the tip of the lateral malleolus, and radiographic studies have found that os subfibulare occurs in 2.1 % of individuals [5]. Considering the relative rarity of the os subfibulare, it has

✉ Jang Gyu Cha
  mj4907@schmc.ac.kr

1 Department of Radiology, Soonchunhyang University Bucheon Hospital, 170 Jomaru-ro, Wonmi-gu, Bucheon-si 14584, Korea

2 Department of Orthopedics, Soonchunhyang University Bucheon Hospital, 170 Jomaru-ro, Wonmi-gu, Bucheon-si 14584, Korea

3 Department of Biomedical Statistics, Soonchunhyang University Bucheon Hospital, 170 Jomaru-ro, Wonmi-gu, Bucheon-si 14584, Korea

4 Division of Rheumatology, Department of Internal Medicine, Soonchunhyang University Bucheon Hospital, 170 Jomaru-ro, Wonmi-gu, Bucheon-si 14584, Korea

🙆 Springer

been suggested that most ossicles adjacent to the lateral malleollus are non-united avulsion fractures that may or may not be associated with ATFL injury or with another traumatic event [6].

For ligamentous or cartilage lesions, magnetic resonance imaging (MRI) is widely used in the diagnosis to plan appropriate treatment, which may prevent the development of osteoarthritis. Most institutions perform ankle MRI with a section thickness of 3–4 mm [7–11]. This may lead to a partial volume effect, however, which may hinder the detection of ankle pathologies. Several recent studies reported low sensitivity for the diagnosis of ligamentous injuries of the ankle joint [10, 11].

Three-dimensional (3D) isotropic MRI has been used for musculoskeletal imaging, including of the shoulder, knee and ankle joints. Use of 3D isotropic sequences enables MR images to be obtained with thinner sections and also enables multiplanar reformation in arbitrary planes that may be tailored to the anatomical structures of interest, which allows us to reduce partial volume averaging effects [12–14]. Several studies of the shoulder and knee joints have used 3D fast spin-echo (FSE) sequences and showed comparable diagnostic performances to two-dimensional (2D) sequences; most revealed higher area under the receiver operating characteristic curve (AUC) values with 2D sequences [15–19].

To the best of our knowledge, there have been no comparisons of the diagnostic performance of 3D isotropic T2-weighted FSE sequences and 2D T2-weighted FSE sequences for the assessment of ATFL, CLT and os subfibulare/avulsion fracture of the distal fibula (OSF), which commonly accompany ankle injuries. The aim of this study was to investigate the diagnostic performance of 3D T2-weighted FSE sequences for the assessment of ATFL tears, CLTs and OSF compared with 2D T2-weighted FSE sequences.

Materials and Methods

Subjects

Between November 2013 and July 2014, a total of 43 consecutive patients with ankle inversion injury who underwent arthroscopy surgery were analyzed. Among them, two patients did not undergo preoperative ankle MRI, and six underwent preoperative ankle MRI without a 3D isotropic T2-weighted FSE sequence. In total, 35 patients were enrolled in our study, comprising 22 women (aged 17–54 years; mean age, 37 years) and 13 men (aged 17–54 years; mean age, 34 years). The mean interval between ankle discomfort and MR imaging was 18 months (although the range was between 7 days and 10 years).

The Institutional Review Board approved the research protocol and waived the requirement for patient informed consent because the study was retrospective in nature.

Imaging study

All images were acquired using a 3.0-T MRI unit (Signa HDx; GE Healthcare, Milwaukee, WI, USA) with an eight-channel boot coil (GE Healthcare), which looks like a ski boot and covers the foot from the ankle to the toes.

Two-dimensional T2-weighted FSE images for comparison with reformats of the 3D sequence were acquired in the axial, sagittal and coronal planes. Imaging with a 3D T2-weighted FSE sequence (Cube, GE Healthcare) was used with a slice thickness of 1 mm in the sagittal plane and without fat suppression. The parameters used for these imaging protocols are listed in Table 1.

Image interpretation

Two musculoskeletal radiologists (one with 14 years of experience and the other with 1 year of experience) who were blinded to the surgical findings evaluated each of 2D and 3D MR images retrospectively and independently. To minimize possible memory of former images, each set of MR images was reviewed with at least a 2-week interval between sessions of interpretation.

Multiplanar reformation of the 3D T2-weighted FSE images with 0.5-mm-thick slices and no interslice gap was carried out using the Aquarius iNtuition software package (ver. 4.4.11; TeraRecon, Inc., San Mateo, CA, USA). According to the orientation of the anterior talofibular ligament and OSF, the images were reformatted using double oblique multiplanar reformation, beginning in the standard axial plane at the level of the ATFL, moving first the plane in the direction parallel to the axis of ATFL, then in the oblique sagittal image, relocating the plane parallel to the axis of the ATFL, the oblique axial (see Fig. 1a). The images were reformatted into oblique sagittal and oblique coronal planes according to the orientation of the dome of the talus (see Fig. 1b).

Readers interpreted the ATFL as a complete tear when there was complete discontinuity, i.e., detachment from the tibial or talar attachment site, and interpreted the ATFL as a partial tear when there were patterns including discontinuity, detachment, thickening, thinning, wavy or irregular contours, and an intermediate or high signal intensity of the ATFL on the MR image with no evidence of a complete tear [20, 21]. Readers simply evaluated the presence or absence of the CLT, increased signal intensity, irregularity of the chondral surface, and detachment of cartilage from the

Table 1 Magnetic resonance imaging (MRI) parameters

Parameter	3D T2-weighted FSE	2D T2-weighted FSE		
		Axial	Sagittal	Coronal
Repetition time (ms)	2500	3707	4155	4966
Echo time (ms)	101	92	87	88
Matrix number	320 × 320	384 × 256	384 × 256	384 × 256
Field of view (cm)	14	14	14	14
Number of acquisition	1	2	0.5	0.5
Echo train length	100	16	12	12
Section thickness (mm)	1	2	3	3
Intersection gap (mm)		1	0.3	0.3
Bandwidth (kHz/pixel)	62.50	41.67	41.67	41.67
Fat suppression	No	No	Yes	Yes
Acquisition time	8 min 30 s	1 min 43 s	1 min 44 s	2 min 5 s
		Sum of time: 5 min 32 s		

talus with or without subchondral bone marrow edema, and described the location of the CLT to compare it with the arthroscopic findings.

A separated ossicle below the lateral malleolus was evaluated to detect OSF, regardless of the ATFL injury.

The same diagnostic criteria were applied to data sets obtained using both the 2D T2-weighted FSE and 3D isotropic T2-weighted FSE sequences.

False-positive and -negative cases for each set of 2D and 3D sequences were re-evaluated by the same two readers who initially evaluated the ankle lesions until a consensus was reached.

Arthroscopic ankle surgery

Arthroscopic findings were considered as the reference standard. Surgeries were carried out by one orthopedic surgeon (Y.K.L, with 9 years of experience, foot and ankle specialist) who could assess the MRI findings before surgery. The surgeon recorded the abnormalities as ATFL, CLT and OSF. The
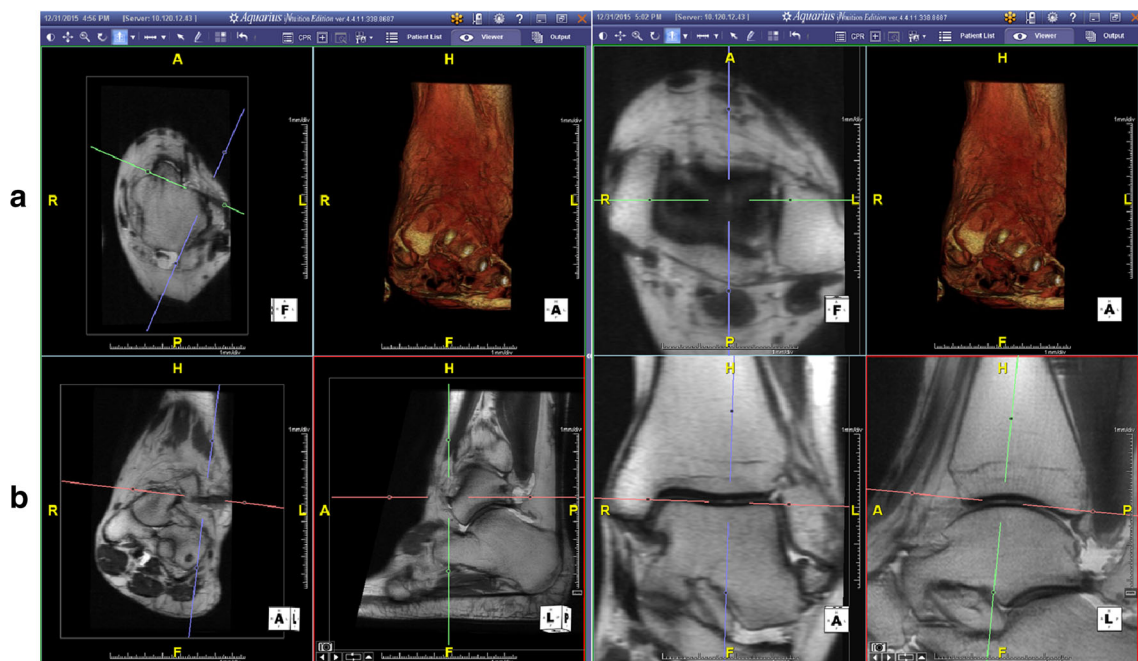
Fig. 1 Screen images from Aquarius iNtuition (version 4.4.11, TeraRecon). **a** Oblique axial plane (left upper quadrant), oblique coronal plane (left lower quadrant) and oblique sagittal plane (right lower quadrant) of the ATFL are obtained to evaluate the degree of injury. **b** Oblique coronal plane (left lower quadrant) and oblique sagittal plane (right lower quadrant) are obtained perpendicular to the articular surface of talar dome

diagnostic criteria for determining AFTL injury were as follows: abnormal course of the ligament, a decrease in the tautness of the ligament, discontinuity of the ligament with or without the defect being filled by fibrous tissue, and an avulsion at the attachment of the fibula or talus [7, 8, 22]. If ATFL injury was noted, the surgeon determined whether the ligament was disrupted completely or partially. A partial tear was defined as thinned, elongated or both, and a complete tear was defined as a definite discontinuity of the ligament and adhesion of adjacent tissue [23]. CLT was noted when there were abnormalities including a rough surface, fibrillation of the articular cartilage and a flap or displaced fragment of the articular cartilage. The surgeon also recorded the location of CLT to compare with MRI findings. The presence or absence of OSF was confirmed by palpation with the probe. The mean time between MRI and arthroscopic surgery was 8.8 days (range: 1 day to 4 months).

Statistical analysis

McNemar's paired proportion test was used to measure the concordance between 2D and 3D sequences and arthroscopic diagnosis [24].

To assess diagnostic performance, the sensitivity, specificity and accuracy of the 3D isotropic T2-weighted FSE and conventional 2D T2-weighted FSE sequences were calculated in relation to the surgical diagnosis. The AUC was compared to determine the discriminatory power of the two image sequences using a nonparametric method [24].

Interobserver agreement was calculated using Cohen's kappa test, where $\kappa < 0$ indicates no agreement, $0 < \kappa \leq 0.2$ indicates slight agreement, $0.2 < \kappa \leq 0.4$ indicates fair agreement, $0.4 < \kappa \leq 0.6$ indicates moderate agreement, $0.6 < \kappa \leq 0.8$ indicates substantial agreement, and $0.8 < \kappa \leq 1$ indicates almost perfect agreement [25].

A significance level of 0.05 was assigned, and 95 % confidence intervals were computed from binomial distributions using Wilson's method [26]. McNemar's paired proportion test, the sensitivity, specificity and accuracy of the 3D and 2D sequences were implemented using R software (ver. 3.1.3), which is freely available from http://cran.r-project.org/, and the AUC was calculated using STATA (ver. 11.0; STATA, College Station, TX, USA).

Results

The analyses of the 2D and 3D sequence images by two readers were compared to the operative findings (see Table 2).

ATFL tear According to the arthroscopy findings, all patients exhibited ATFL tears: 21 complete tears and 14 partial tears of the ATFL were revealed from the arthroscopic surgery. In total, 7 of the 21 complete tears were accompanied by OSF, and the others were not associated with OSF. Table 3 lists the AUC values representing the diagnostic performance of the 3D T2-weighted FSE and 2D T2-weighted FSE sequences. We found higher AUC values for the 3D sequence than the 2D sequence for both readers (Figure 2 provides an example of a true-positive ATFL tear, which was discordant between 2D and 3D sequence images); however, the differences between the diagnoses from the 2D and 3D T2-weighted FSE sequences from both of the two readers were not statistically significant for the diagnosis of ATFL tears (reader A, $p = 0.50$; reader B, $p = 0.07$). Table 4 lists the sensitivity, specificity and accuracy of the diagnoses obtained using the two sequences.

There was one overestimated case of a partial tear of the ATFL on the arthroscopy finding, which was interpreted as a complete tear by both readers in the 3D sequence. However, following a second viewing of the MR images, the residual quarter-thickness of ATFL was found at the fibular attachment site. There were two underestimated cases of complete tears of the ATFL from the arthroscopy, which were interpreted as partial tears by both readers in both sequences. Following a second viewing of the MR images, one case was interpreted as thinning of the ATFL at the mid portion, with increased signal intensity but preserved continuity, and the other exhibited thickened ATFL without increased signal intensity and complete detachment at the fibular attachment site.

CLT From the arthroscopic findings, 17 (48.57 %) of the 35 patients had CLT. Table 3 lists the AUC values representing the diagnostic performance of the 3D T2-weighted FSE sequences versus those of 2D T2-weighted FSE sequences (Figure 3 provides an example of true-positive CLT on the 3D sequence image, which was not definite on the 2D sequence image). There were no significant differences in the diagnoses of CLT obtained from the 2D and 3D sequences by either reader (reader A, $p = 0.09$; reader B, $p = 0.45$). There was a trend toward higher AUC values from the 3D sequences than the 2D sequences for both readers. Table 4 lists the sensitivity, specificity and accuracy of the two sequences. There were six false-negative cases of no lesion from the 2D sequences, as diagnosed by both readers. However, there were no false-negative cases from the 3D sequences that were interpreted as no lesion by both readers. Two false-positive cases were noted by both readers using the 3D sequences, and there were no false-positive cases using the 2D sequences. We retrospectively reviewed the false-positive/-negative cases of both readers compared with the arthroscopic findings; the results were as follows: (1) true false-positive lesions without correlating lesions (n = 2); (2) interpreted as CLT by both readers A and B, but arthroscopy revealed only synovitis (n = 3); (3) minimal damage (fraying) observed during arthroscopy, which was not considered significant, although one lesion appeared as subchondral bone marrow edema on the MR

Table 2 Comparisons of MRI and operative finding for both readers

		2D T2-weighted FSE		3D T2-weighted FSE		Operation
		Reader A	Reader B	Reader A	Reader B	
ATFL	CT	19 (54 %)	12 (34 %)	22 (63 %)	17 (49 %)	21 (60 %)
	PT	16 (46 %)	23 (66 %)	13 (37 %)	18 (51 %)	14 (40 %)
CLT	Present	8 (23 %)	8 (23 %)	23 (66 %)	16 (46 %)	17 (49 %)
	Absence	27 (77 %)	27 (77 %)	12 (34 %)	19 (54 %)	18 (51 %)
OSF	Present	13 (37 %)	11 (31 %)	12 (34 %)	13 (37 %)	7 (20 %)
	Absence	22 (63 %)	24 (69 %)	23 (66 %)	22 (63 %)	28 (80 %)

Abbreviations: CT, complete tear; PT, partial tear; ATFL, anterior talofibular ligament; CLT, chondral lesion of the talus; OSF, os subfibulare/avulsion fracture of the distal fibula

Data are listed as the number of subjects, with the percentage of the total sample of 35 in parentheses

Reader A: musculoskeletal radiologist with 1 year of experience

Reader B: musculoskeletal radiologist with 14 years of experience

images (n = 4); (4) lesions located in the lateral aspect of the talus below Basset's ligament on arthroscopy, which were not identified on the MR images (n = 2).

OSF From the arthroscopy, 7 (20 %) of the 35 patients exhibited OSF. Table 3 lists the AUC values representing the diagnostic performance of 3D T2-weighted FSE sequences versus that of 2D T2-weighted FSE sequences. There was no statistically significant difference ($p = 0.32$) in the diagnosis of OSF between the 2D FSE and 3D FSE sequences for either reader. Table 4 lists the sensitivity, specificity and accuracy. Four cases were considered as positive by both of two readers on both 2D and 3D sequences, but negative from the arthroscopic findings (Figure 4 provides an example of OSF detected by both sequences but not found on the arthroscopic findings). No false-negative cases were noted from either the 3D or 2D sequences.

Interobserver agreement was substantial for chondral lesions of the talus ($\kappa = 0.676$) and OSF ($\kappa = 0.621$) via the 2D T2-weighted FSE sequence and for ATFL ($\kappa = 0.659$) and OSF ($\kappa = 0.689$) via the 3D T2-weighted FSE sequence. Interobserver agreement was moderate for CLT ($\kappa = 0.499$) via the 3D T2-weighted FSE sequence and for ATFL ($\kappa = 0.553$) via the 2D T2-weighted FSE sequence.

Discussion

The ATFL is the most commonly injured ligament following lateral ankle injury [2, 27]. We used an ATFL injury classification system that was modified from the grade system of the American Medical Association and Cass *et al.*, whereby grade I corresponds to the ligament

Table 3 Comparison of the area under the curve (AUC) values of 2D T2-weighted fast spin-echo (FSE) and 3D T2-weighted FSE sequences for both readers

	2D T2-weighted FSE	3D T2-weighted FSE	Difference*	*p*-value
ATFL				
Reader A	0.774 (0.628, 0.919)	0.821 (0.686, 0.957)	0.047 (−0.088, 0.184)	0.501
Reader B	0.690 (0.545, 0.835)	0.845 (0.729, 0.962)	0.155 (−0.026, 0.310)	0.074
CLT				
Reader A	0.678 (0.546, 0.810)	0.833 (0.721, 0.945)	0.155 (−0.016, 0.334)	0.090
Reader B	0.735 (0.613, 0.858)	0.799 (0.662, 0.936)	0.064 (−0.105, 0.227)	0.450
OSF				
Reader A	0.893 (0.815, 0.970)	0.911 (0.838, 0.983)	0.018 (−0.029, 0.036)	0.317
Reader B	0.929 (0.863, 0.995)	0.893 (0.815, 0.970)	0.036 (−0.107, 0.037)	0.317

Abbreviations: ATFL, anterior talofibular ligament; CLT, chondral lesion of the talus; OSF, os subfibulare/avulsion fracture of the distal fibula

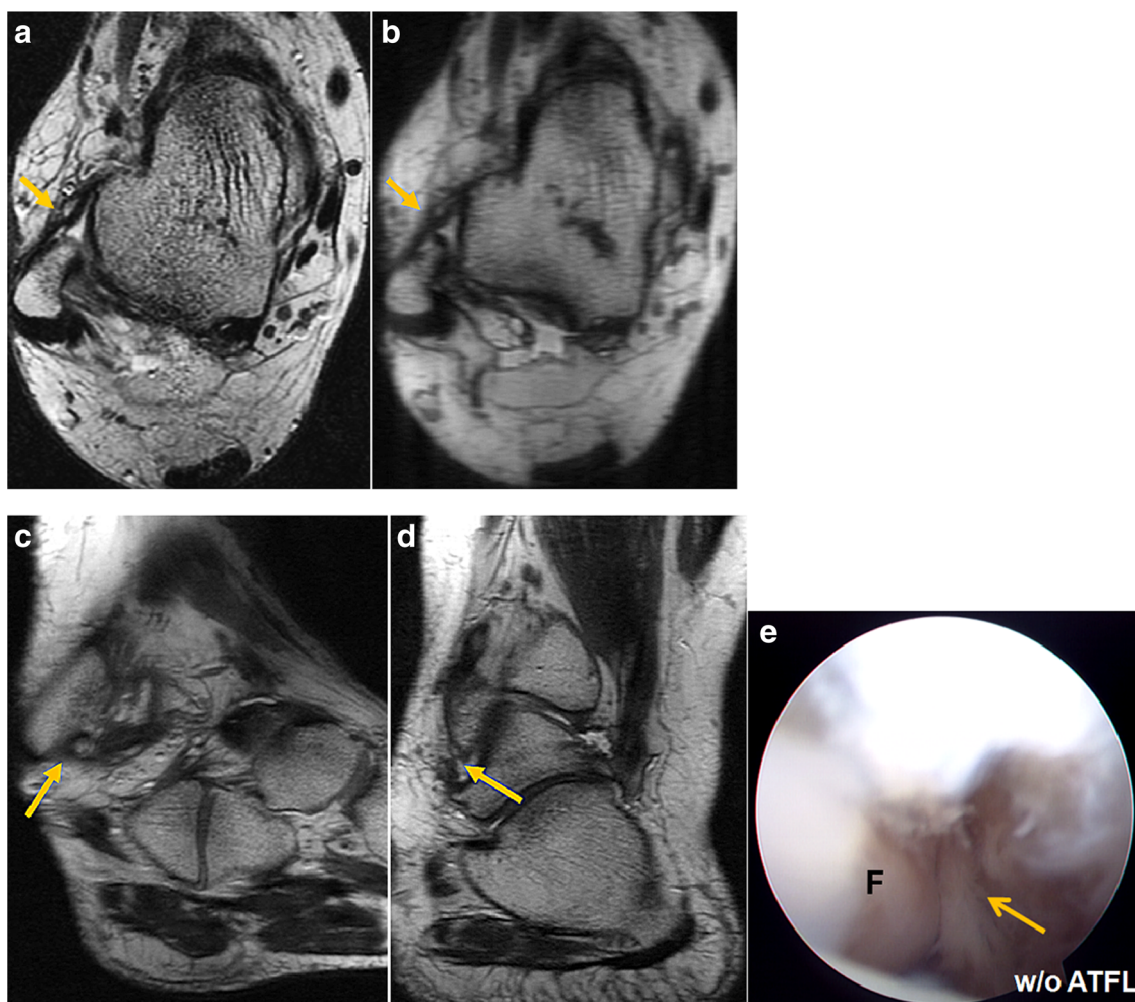Data are presented as parameters with 95 % confidence intervals in parentheses

*Data are mean differences in AUC scores between the 2D T2-weighted FSE group and the 3D T2-weighted FSE group

P-values for the comparison of AUC were calculated using Delong's method

Fig. 2 Anterior talofibular ligament (ATLF) tear. True positive and discordant between 2D and 3D sequence images. A 53-year-old female with ankle discomfort. A thinning, wavy contour of the ATFL was noted from the two-dimensional (2D) T2 fast spin-echo (FSE) sequence image (**a**). Both readers considered this as a partial tear from the 2D T2 FSE image. From the three-dimensional (3D) T2 FSE sequence MR image, disruption at the fibula attachment site of the ATFL was detected (**b–d**), and both readers interpreted this as a complete tear. Arthroscopy confirmed it as a complete tear (**e**)

being stretched with no tearing, laxity and little pain; grade II corresponds to a partial tear of the ligament, with minimal laxity and moderate pain; and grade III corresponds to complete rupture of the ligament, with instability of the joint [20, 21]. In other words, grade I and II lesions are partial tears, and grade III lesions are complete tears. We focused on the diagnostic performance for differentiating complete tears from partial tears, which has clinical importance because treatment plans for grade I and grade II ligament injuries are conservative, whereas those for grade III injuries are controversial between functional treatment (including early mobilization, cast immobilization, pharmacological, physical therapy and intrajoint injection) and primary surgical repair [21, 28]. Conventional ankle MRI commonly includes several 2D-FSE sequences acquired in orthogonal scan planes [14]. We hypothesized that

the diagnostic performance for ATFL tears would be higher for the 3D T2-weighted FSE sequence than the 2D T2-weighted FSE sequence, whereby the data were acquired in thin sections. Although there was no statistical significance, we found higher AUC values in the diagnosis of ATFL tears using the 3D T2-weighted FSE sequence than the 2D T2-weighted FSE sequence. This is not consistent with previous study on the shoulder joint, which reported higher AUC values for 2D sequences than 3D sequences [15]. There are a number of possible reasons for this. First, the ankle joint is smaller than the shoulder joint, so the scan time is shorter for the ankle joint, which may reduce the possibility of motion artifacts during the scan [15, 29]. Second, the ankle joint is not affected by breathing motion artifacts, unlike the shoulder joint [30]. Decreased effects of motion artifacts may explain the higher AUC

Table 4 Sensitivity, specificity and accuracy of 2D FSE and 3D FSE sequences in the detection of ATFL lesions, CLT and OSF

	Reader A		Reader B	
	2D T2-weighted FSE	3D T2-weighted FSE	2D T2-weighted FSE	3D T2-weighted FSE
ATFL				
Sensitivity	0.76 (0.53–0.92)	0.86 (0.64–0.97)	0.52 (0.30–0.74)	0.76 (0.53–0.92)
Specificity	0.79 (0.49–0.95)	0.79 (0.49–0.95)	0.86 (0.57–0.98)	0.93 (0.66–1.00)
Accuracy	0.77 (0.60–0.90)	0.83 (0.66–0.93)	0.66 (0.48–0.81)	0.83 (0.66–0.93)
CLT				
Sensitivity	0.41 (0.18–0.67)	1.00 (0.73–1.00)	0.47 (0.23–0.72)	0.76 (0.50–0.93)
Specificity	0.94 (0.73–1.00)	0.67 (0.41–0.87)	1.00 (0.74–1.00)	0.83 (0.59–0.96)
Accuracy	0.69 (0.51–0.83)	0.83 (0.66–0.93)	0.74 (0.57–0.88)	0.80 (0.63–0.92)
OSF				
Sensitivity	1.00 (0.47–1.00)	1.00 (0.47–1.00)	1.00 (0.47–1.00)	1.00 (0.47–1.00)
Specificity	0.79 (0.59–0.92)	0.82 (0.63–0.94)	0.86 (0.67–0.96)	0.79 (0.59–0.92)
Accuracy	0.83 (0.66–0.93)	0.86 (0.70–0.95)	0.89 (0.73–0.97)	0.83 (0.66–0.93)

Abbreviations: ATFL, anterior talofibular ligament; CLT, chondral lesion of the talus; OSF, os subfibulare/avulsion fracture of the distal fibula

Data are presented as parameters with 95 % confidence intervals in parentheses

values for the 3D sequence than the 2D sequence. Third, when 2D-FSE sequences are acquired using thicker slices and/or slice gaps, this may lead to problems in detecting ankle pathologies such as ligament tears or cartilage injuries [14].

Chondral lesions usually occur in the talar dome. Frequent sites of CLT are the middle third of the lateral border and the posterior third of the medial border [3]. High-resolution techniques with thin sections and differential contrast among hyaline cartilage, subchondral bone and joint fluid are crucial for evaluating cartilage lesions [31]. We found that the 3D T2-weighted FSE sequence resulted in higher AUC values, sensitivity and accuracy for detecting CLT than the 2D T2-weighted FSE sequence. This result is consistent with a previous study on chondromalacia of the knee joint [32, 33]. However, the sensitivity of the 2D sequence for detecting osteochondral lesions of the talus (41–47 %) was lower than that previously reported (95 %), in which grade-I lesions were considered normal because of the lack of clinical significance [31]. Given that our study included superficial articular lesions (which were excluded in the previous study [37]), this may be the reason for the lower sensitivity observed in our study. We found that the 3D sequence showed a slightly higher trend of sensitivity than the 2D sequence in the detection of CLT. Though the higher trend of sensitivity for 3D sequence is offset by lower specificity, we expect that 3D FSE may show similar diagnostic performance to 2D FSE for detecting cartilage lesions, allowing for thin sections and arbitrary planes according to the anatomical structures of interest [33].

The accuracy of diagnosing OSF was 69–84 %. The sensitivity, specificity and accuracy for detection of OSF were similar between 2D and 3D sequences. It is not surprising that OSF was not detected via arthroscopy, because arthroscopic surgery is limited to a narrow search over a small region of the ankle joint. Furthermore, OSFs are likely to be hidden by synovitis or inflammatory granulation tissue and so may not be detected by arthroscopy, especially when OSFs are not completely retracted from the mother bone. Examining MR images prior to planning surgery may help in detecting OSFs.
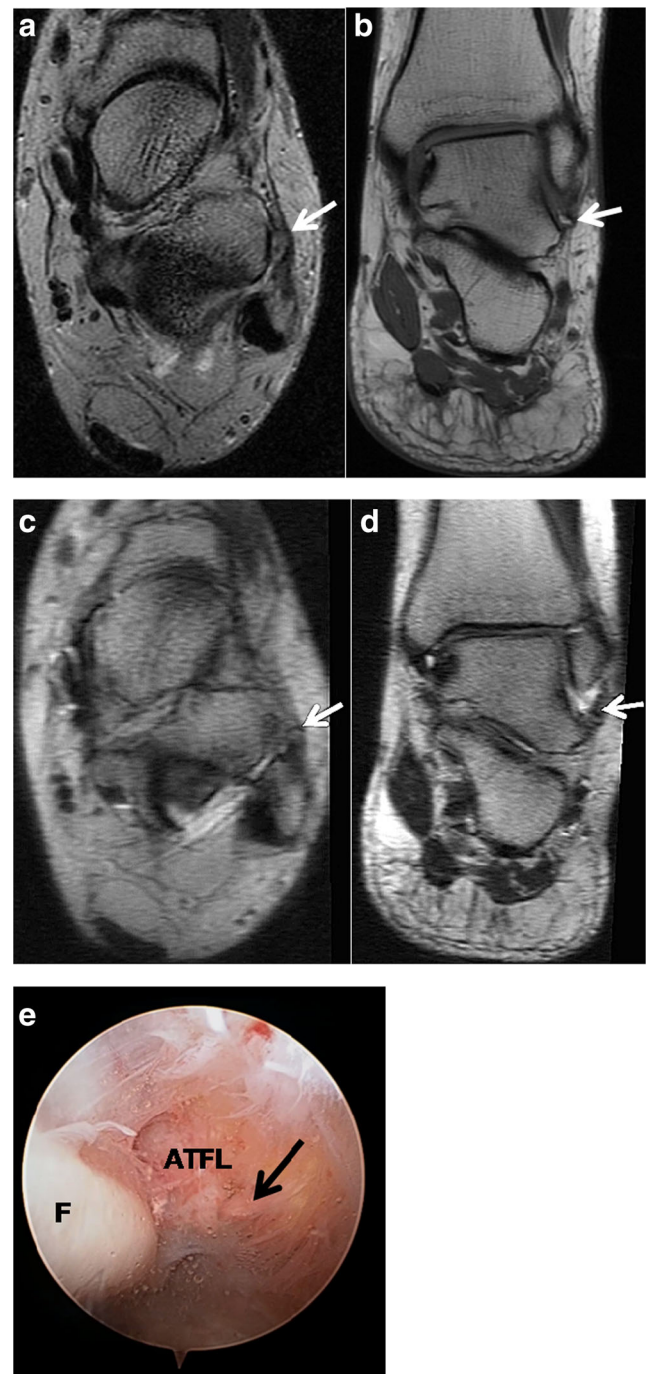
Limitations

This study had several limitations. First, we did not include a control group without complaints of the ankle joint, including instability, and only included patients who underwent arthroscopic surgery, which may have led to selection bias. However, it is neither practically nor ethically feasible to perform invasive ankle arthroscopy for healthy volunteers. Second, most patients underwent ankle MRI after months or years of discomfort; in the chronic stage of an ATFL tear, the gap in the torn ATFL ligament is replaced by scar tissue or fibrosis, and remodeling to the normal thickness may occur [34]. This might have contributed to lower sensitivity for detection of ATFL tears. Third, we did not apply parallel imaging to the 3D isotropic sequence, and more time was required to acquire the 3D-isotropic-sequence images (8 min and 30 s) than the
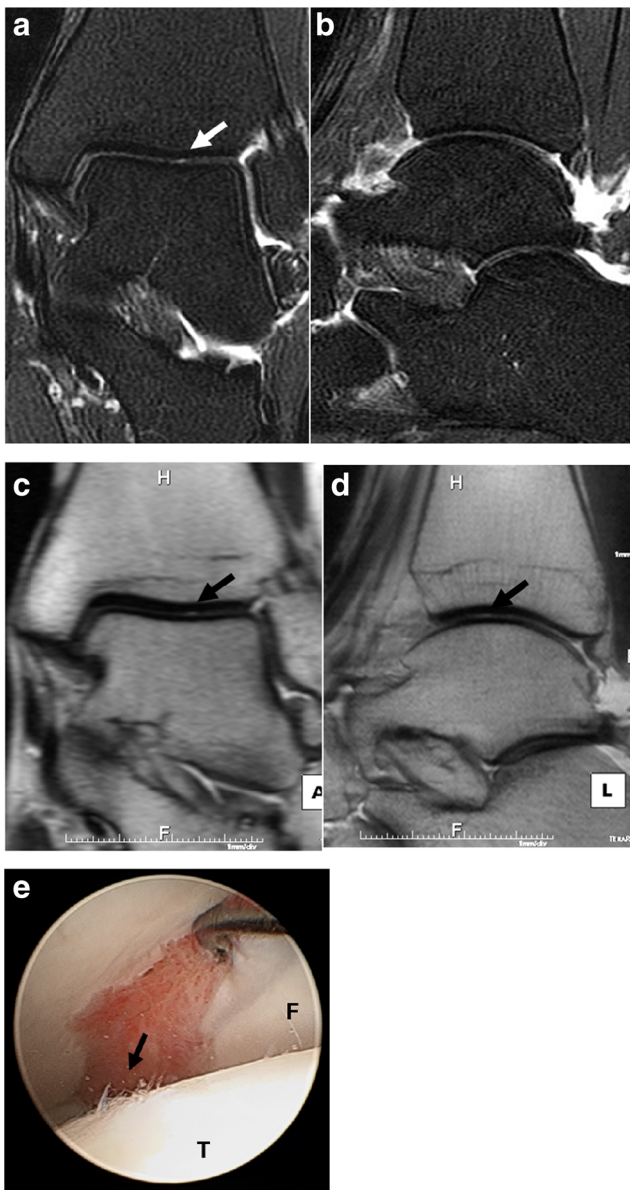
Fig. 3 Chondral lesion of the talus (CLT). False negative on 2D and true positive on 3D, and discordant between 2D and 3D sequence images. A 35-year-old female with ankle discomfort. Focal cartilage defect was suspected from the 2D coronal T2 FSE image (a), but was not definite on the sagittal plane (b). One reader considered this a positive finding, but the other considered it a negative finding. The 3D T2 FSE coronal and sagittal reconstructed images (c, d) clearly show the focal high signal portion in the dome of the talus (see the arrow), and both readers interpreted this as a positive finding. Arthroscopy confirmed CLT (e)

Fig. 4 Os subfibulare. True positive and concordant between 2D and 3D sequence images. A 44-year-old female patient with ankle discomfort for 2 months. A small osseous lesion was noted below the distal fibula on both the 2D and 3D sequence images (a–d). Arthroscopy revealed a complete tear of the ATFL, together with adhesion and fibrosis, which may have obscured the osseous lesion (e)

conventional 2D sequence images (5 min and 32 s). Through the use of parallel imaging, 3D isotropic spin-echo images can be obtained with shorter image scan times and a more flexible protocol design [35, 36]. Fourth, though the arthroscopy finding could not detect all OSFs, it was used as a reference standard to confirm the presence or absence of OSF. It might also potentially lower the specificity and accuracy for diagnosing OSF.

To the best of our knowledge, this work represents the first study comparing the diagnostic performance of 3D T2-weighted FSE and 2D conventional FSE sequences for ATFL tears, CLTs and OSFs. Further study to support the results of this work is required.

Conclusion

Three-dimensional isotropic T2-weighted FSE MRI of the ankle resulted in no statistically significant difference in diagnostic performance compared to two-dimensional T2-weighted FSE MRI in the evaluation of ATFL tears, chondral lesions of the talus and OSFs.

References

1. Fong DT, Hong Y, Chan LK, Yung PS, Chan KM. A systematic review on ankle injury and ankle sprain in sports. Sports Med. 2007;37(1):73–94.
2. Erickson SJ, Smith JW, Ruiz ME, et al. MR imaging of the lateral collateral ligament of the ankle. AJR Am J Roentgenol. 1991;156(1):131–6.
3. Flick AB, Gould N. Osteochondritis dissecans of the talus (transchondral fractures of the talus): review of the literature and new surgical approach for medial dome lesions. Foot Ankle. 1985;5(4):165–85.
4. Buckwalter JA, Mow VC, Ratcliffe A. Restoration of injured or degenerated articular cartilage. J Am Acad Orthop Surg. 1994;2(4):192–201.
5. Tsuruta T, Shiokawa Y, Kato A, et al. Radiological study of the accessory skeletal elements in the foot and ankle (author's transl). Nihon Seikeigeka Gakkai Zasshi. 1981;55(4):357–70.
6. Berg EE. The symptomatic os subfibulare. Avulsion fracture of the fibula associated with recurrent instability of the ankle. J Bone Joint Surg Am. 1991;73(8):1251–4.
7. Takao M, Innami K, Matsushita T, Uchio Y, Ochi M. Arthroscopic and magnetic resonance image appearance and reconstruction of the anterior talofibular ligament in cases of apparent functional ankle instability. Am J Sports Med. 2008;36(8):1542–7.
8. Oae K, Takao M, Uchio Y, Ochi M. Evaluation of anterior talofibular ligament injury with stress radiography, ultrasonography and MR imaging. Skelet Radiol. 2010;39(1):41–7.
9. Cha SD, Kim HS, Chung ST, et al. Intra-articular lesions in chronic lateral ankle instability: comparison of arthroscopy with magnetic resonance imaging findings. Clin Orthop Surg. 2012;4(4):293–9.
10. Lee MH, Cha JG, Lee YK, et al. The bright rim sign on MRI for anterior talofibular ligament injury with arthroscopic correlation. AJR Am J Roentgenol. 2012;198(4):885–90.
11. Park HJ, Cha SD, Kim SS, et al. Accuracy of MRI findings in chronic lateral ankle ligament injury: comparison with surgical findings. Clin Radiol. 2012;67(4):313–8.
12. Yao L, Pitts JT, Thomasson D. Isotropic 3D fast spin-echo with proton-density-like contrast: a comprehensive approach to musculoskeletal MRI. AJR Am J Roentgenol. 2007;188(2):W199–201.
13. Stevens KJ, Busse RF, Han E, et al. Ankle: isotropic MR imaging with 3D-FSE-cube—initial experience in healthy volunteers. Radiology. 2008;249(3):1026–33.
14. Stevens KJ, Wallace CG, Chen W, Rosenberg JK, Gold GE. Imaging of the wrist at 1.5 Tesla using isotropic three-dimensional fast spin echo cube. J Magn Reson Imaging. 2011;33(4):908–15.
15. Choo HJ, Lee SJ, Kim OH, Seo SS, Kim JH. Comparison of three-dimensional isotropic T1-weighted fast spin-echo MR arthrography with two-dimensional MR arthrography of the shoulder. Radiology. 2012;262(3):921–31.
16. Jung JY, Jee WH, Park MY, Lee SY, Kim YS. SLAP tears: diagnosis using 3-T shoulder MR arthrography with the 3D isotropic turbo spin-echo space sequence versus conventional 2D sequences. Eur Radiol. 2013;23(2):487–95.
17. Kloth JK, Winterstein M, Akbar M, et al. Comparison of 3D turbo spin-echo SPACE sequences with conventional 2D MRI sequences to assess the shoulder joint. Eur J Radiol. 2014;83(10):1843–9.
18. Lee JH, Yoon YC, Jee S, Kwon JW, Cha JG, Yoo JC. Comparison of three-dimensional isotropic and two-dimensional conventional indirect MR arthrography for the diagnosis of rotator cuff tears. Korean J Radiol. 2014;15(6):771–80.
19. Park SY, Lee IS, Park SK, Cheon SJ, Ahn JM, Song JW. Comparison of three-dimensional isotropic and conventional MR arthrography with respect to the diagnosis of rotator cuff and labral lesions: focus on isotropic fat-suppressed proton density and VIBE sequences. Clin Radiol. 2014;69(4):e173–82.
20. Cass JR, Morrey BF. Ankle instability: current concepts, diagnosis, and treatment. Mayo Clin Proc. 1984;59(3):165–70.
21. DeLee JC, Drez D, Miller MD, et al. DeLee & Drez's orthopaedic sports medicine: principles and practice. Volume Two: Saunders; 2003.
22. Frey C, Bell J, Teresi L, Kerr R, Feder K. A comparison of MRI and clinical examination of acute lateral ankle sprains. Foot Ankle Int. 1996;17(9):533–7.
23. Marder RA. Current methods for the evaluation of ankle ligament injuries. Instr Course Lect. 1995;44:349–57.
24. DeLong ER, DeLong DM, Clarke-Pearson DL. Comparing the areas under two or more correlated receiver operating characteristic curves: a nonparametric approach. Biometrics. 1988;44(3):837–45.
25. Landis JR, Koch GG. The measurement of observer agreement for categorical data. Biometrics. 1977;33(1):159–74.
26. Wilson EB. Probable inference, the law of succession, and statistical inference. J Am Stat Assoc. 1927;22(158):209–12.
27. Campbell SE, Warner M. MR imaging of ankle inversion injuries. Magn Reson Imaging Clin N Am. 2008;16(1):1–18. v.
28. Ardevol J, Bolibar I, Belda V, Argilaga S. Treatment of complete rupture of the lateral ligaments of the ankle: a randomized clinical trial comparing cast immobilization with functional treatment. Knee Surg Sports Traumatol Arthrosc. 2002;10(6):371–7.
29. Jung JY, Yoon YC, Kwon JW, Ahn JH, Choe BK. Diagnosis of internal derangement of the knee at 3.0-T MR imaging: 3D isotropic intermediate-weighted versus 2D sequences. Radiology. 2009;253(3):780–7.
30. Dietrich TJ, Ulbrich EJ, Zanetti M, Fucentese SF, Pfirrmann CW. PROPELLER technique to improve image quality of MRI of the shoulder. AJR Am J Roentgenol. 2011;197(6):W1093–100.
31. Mintz DN, Tashjian GS, Connell DA, Deland JT, O'Malley M, Potter HG. Osteochondral lesions of the talus: a new magnetic resonance grading system with arthroscopic correlation. Arthroscopy. 2003;19(4):353–9.
32. Jung JY, Yoon YC, Kim HR, Choe BK, Wang JH, Jung JY. Knee derangements: comparison of isotropic 3D fast spin-echo, isotropic 3D balanced fast field-echo, and conventional 2D fast spin-echo MR imaging. Radiology. 2013;268(3):802–13.

33. Kijowski R, Davis KW, Woods MA, et al. Knee joint: comprehensive assessment with 3D isotropic resolution fast spin-echo MR imaging—diagnostic performance compared with that of conventional MR imaging at 3.0 T. Radiology. 2009;252(2):486–95.

34. Chan KW, Ding BC, Mroczek KJ. Acute and chronic lateral ankle instability in the athlete. Bull NYU Hosp Jt Dis. 2011;69(1):17–26.

35. Glockner JF, Hu HH, Stanley DW, Angelos L, King K. Parallel MR imaging: a user's guide 1. Radiographics. 2005;25(5):1279–97.

36. Bauer JS, Banerjee S, Henning TD, Krug R, Majumdar S, Link TM. Fast high-spatial-resolution MRI of the ankle with parallel imaging using GRAPPA at 3 T. AJR Am J Roentgenol. 2007;189(1):240–5.